energies

MDPI

Article

Investigating the Drying Process of Ceramic Sanitary Ware at Low Temperature

Ricardo S. Gomez [1], Kelly C. Gomes [1,2], José M. A. M. Gurgel [1,2], Laís B. Alves [3], Hortência L. F. Magalhães [4], Raíssa A. Queiroga [1], Gustavo C. P. Sousa [1], Aline S. Oliveira [1], Anderson F. Vilela [5], Bruna T. A. Silva [6], Danielle B. T. Vasconcelos [7], Glauco R. F. Brito [8] and Antonio G. B. Lima [8,*]

1 Postgraduate Program in Mechanical Engineering, Federal University of Paraíba, João Pessoa 58051-900, Paraíba, Brazil; ricardosoaresgomez@gmail.com (R.S.G.); gomes@cear.ufpb.br (K.C.G.); josemauriciogurgel@gmail.com (J.M.A.M.G.); raissa.queiroga089@gmail.com (R.A.Q.); pamplonagustavo@hotmail.com (G.C.P.S.); aline.oliveira@cear.ufpb.br (A.S.O.)
2 Department of Renewable Energy Engineering, Federal University of Paraíba, João Pessoa 58051-900, Paraíba, Brazil
3 Dexco S.A, João Pessoa 58082-797, Paraíba, Brazil; lais.belizario@dex.co
4 Science and Technology Institute, Federal University of Jequitinhonha and Mucuri Valleys, Diamantina 39100-000, Minas Gerais, Brazil; hortencia.luma@ufvjm.edu.br
5 Department of Agro-Industrial Management and Technology, Federal University of Paraíba, Bananeiras 58220-000, Paraíba, Brazil; prof.ufpb.anderson@gmail.com
6 Department of Civil Engineering, Federal University of Campina Grande, Campina Grande 58429-900, Paraíba, Brazil; brunathallyta@hotmail.com
7 Federal Institute of Education, Science and Technology of Alagoas, Piranhas 57460-000, Alagoas, Brazil; danielle.silva@ifal.edu.br
8 Department of Mechanical Engineering, Federal University of Campina Grande, Campina Grande 58429-900, Paraíba, Brazil; glaucoruben@hotmail.com
* Correspondence: antonio.gilson@ufcg.edu.br; Tel.: +55-(83)-98771-3209

Citation: Gomez, R.S.; Gomes, K.C.; Gurgel, J.M.A.M.; Alves, L.B.; Magalhães, H.L.F.; Queiroga, R.A.; Sousa, G.C.P.; Oliveira, A.S.; Vilela, A.F.; Silva, B.T.A.; et al. Investigating the Drying Process of Ceramic Sanitary Ware at Low Temperature. *Energies* **2023**, *16*, 4242. https://doi.org/10.3390/en16104242

Academic Editors: Huijin Xu and Guojun Yu

Received: 8 April 2023
Revised: 12 May 2023
Accepted: 19 May 2023
Published: 22 May 2023

Abstract: Drying is one of the stages with the highest energy consumption in the manufacturing process of ceramic materials and aims to reduce the product's moisture to levels necessary for safe firing stage, reducing the chances of defect formation. For sanitary ware, there is an additional energy cost in the pre-drying stage, which takes place immediately after removing the parts from the molds, and is carried out in an environment with lower temperatures (ranging from 30 to 40 °C). This work aims to experimentally study the drying process of sanitary ware at low temperatures, with particular reference to sanitary toilets with industrial dimensions. Four drying experiments were carried out in an oven with different operating conditions (temperature and relative humidity). The results indicate that an increase in temperature and reduction in relative humidity provoke a faster drying rate. For some physical situations, it is more interesting to dedicate efforts to reducing the relative humidity of the drying air instead of seeking solutions to raise its temperature. Furthermore, a correlation between the linear retraction and moisture content was observed; the greater the moisture loss, the greater the sample shrinkage.

Keywords: sanitary toilet; ceramics; clay; heat; mass

1. Introduction

The ceramic industry plays a very important role in the Brazilian economy, with a share of approximately 1% of the national GDP; approximately 40% of this share is represented by red or structural ceramics [1]. According to data from the National Association of the Ceramic Industry (Brazil), this sector is made up of approximately 7000 companies; generating 293,000 direct jobs and 900,000 indirect job; and is responsible for an annual revenue of around R$ 18 billion, which corresponds to about 4.8% of the building industry [2]. As it represents a sector of great importance in job creation and income distribution,

it deserves the attention of government sectors, research institutes, universities and various entities [3].

Ceramic materials have multiple properties that contribute to their wide application in civil construction and engineering: high mechanical strength, high hardness, high melting temperature, high abrasion resistance, high heat resistance, chemical and thermal stability, durability and great thermal and acoustic insulation capacity [1,4,5].

The main steps in the manufacturing process of ceramic materials are exploration, raw material preparation, conformation and thermal processing (drying and firing) [6]. During the raw material preparation stage, water is added to the clay in order to increase its plasticity, allowing the piece to be molded or conformed easily without cracking [7–9]. After molding, the piece must experience the drying stage; this process consists of removing moisture from the porous material through supplying energy (heat) to itself.

In the process of drying ceramic materials, there is heat transfer from the hot air to the material surface via convection, which heats up the material and creates a temperature gradient within it (conduction heat transfer). As the water present in the solid is heated, its vapor pressure increases, creating favorable conditions for migration of water from the interior to the surface of the solid, resulting in the formation of a moisture gradient within the solid. Finally, the water evaporates from the surface and is absorbed through the drying air due to the partial pressure difference of the water vapor between the material surface and the surrounding air, leading to the creation of new temperature and moisture gradients within the solid. This process continues until the hygroscopic equilibrium condition is reached [3].

Drying is considered a very delicate and complex step in the manufacturing process of ceramic materials, as water removal is accompanied by heat transfer, internal stresses arising from temperature and moisture gradients and significant dimensional changes [10,11]. Therefore, it is crucial to carry out this step in a uniform and controlled manner to avoid the formation of cracks, twists, warping and other types of defects or even the explosion of the product in the firing stage [7,12,13].

The drying and firing processes of ceramic products are characterized by high energy consumption [14–16]. Silva et al. [5] reported that the energy cost during the drying and firing stages has a considerable influence on the price of the final product, representing about 30% of the total average cost of production.

When it comes to sanitary ware, the ceramic mass is composed of plastic (clay and kaolin) and non-plastic raw materials (feldspar, phyllite, and quartz) [17]. Generally, non-plastic raw materials are dry ground until they reach the appropriate particle size and are then mixed with plastic raw materials, water and a deflocculant (usually sodium silicate) in tanks with mechanical agitation [4]. The resulting pulp, known as ceramic slip or barbotine, is screened and pumped to the casting sector, where the sanitary pieces are cast in plaster or resin molds [18]. After molding, the pieces experience the stages of pre-drying, drying, glazing and firing, and are then stored and delivered to the customer.

In this way, it is common to have an additional energy cost in the pre-drying stage, which occurs immediately after removing the pieces from the molds. This step consists of keeping the pieces in a large environment with a temperature between 30 and 40 °C for a period ranging from one to three days, depending on the product, to reduce the moisture content of the material for ideal values for the subsequent drying stage. Normally, in the Brazilian industry, a large amount of natural gas is burned to keep such environments in the ideal temperature range for pre-drying.

In the consulted literature, no studies were found that evaluated the drying process of ceramic materials at low temperatures (less than 50 °C). In addition, such works are limited to simpler geometries, such as hollow bricks and ceramic blocks [1,3,5,7,8,13,16,19–35]. It was also noticed that the only operational parameter evaluated in the drying process of ceramic materials reported in the literature is the temperature of the drying air; parameters not being evaluated, for example, were cases involving the same temperature and different values for relative humidity and/or velocity, including dimensions variations. When it

comes to sanitary ware, the works are even more scarce, not even being found experimental drying studies for such products. Therefore, the innovation of the work is evident.

Thus, the motivation for this research is related to the lack of work on drying sanitary ware at low temperatures. Therefore, the aim of this research is to study drying process of sanitary ware with industrial dimensions in the range of 30 to 40 °C. The idea is making it possible to contribute to improving the pre-drying process of products in the ceramic industry sector. From experimental analyzes in an oven, it was possible to study the drying kinetics and linear retraction of sanitary toilets for different values of air temperature and relative humidity. Such results should provide a basis to assist in decision-making aimed at a more efficient pre-drying, either through reducing energy consumption or processing time and quickly reaching the desired moisture content for the product to be submitted to drying in the stages of the manufacturing process.

2. Methodology

2.1. Oven Drying Experiments

Oven drying experiments were carried out with the aim of evaluating the influence of air temperature and relative humidity on the moisture content, temperature and dimensions of the product.

2.1.1. Materials and Equipment Used in the Experiments

The materials used in the oven drying experiments were conventional sanitary toilets (Figure 1), which were kindly provided by the partner company DEXCO S.A (João Pessoa, Brazil). The main dimensions of the part after removal from the mold and before the start of the drying experiments were as follows:

- Height: 430 ± 5 mm;
- Upper part length: 511 ± 2 mm;
- Upper part width: 413 ± 3 mm;
- Bottom part length: 426 ± 2 mm;
- Bottom part width: 220 ± 1 mm.

Figure 1. Sanitary toilet before drying experiment.

To carry out the experiments and determine the drying parameters, the following equipment were used (Figure 2):

(a) Drying oven with temperature controller, circulation and forced air renewal, internal dimensions 50 × 60 × 60 cm (height × width × depth), brand MYLABOR EQUIPAMENTOS, model SSD-180L. The oven's working temperature ranged from 5 to 250 °C.
(b) Digital scale, brand RAMUZA, model DP-35 with a maximum capacity of 35 kg and a resolution of 5 g.
(c) Measuring tape, brand SQ, with a length of 5 m and a tape width of 19 mm for measuring the main dimension of the samples during the drying processes.
(d) Digital thermo-hygrometer, brand KASVI, model K29-5070h for measuring the temperature and relative humidity of the ambient air outside the oven. Accuracy ±0.1 °C and ±1%, respectively.
(e) Digital thermo-hygrometer, brand ICEL, model HT-220 for measuring the temperature and relative humidity of the air inside the oven. Accuracy ±0.1 °C and ±1%, respectively.
(f) Digital infrared thermometer, brand KZED, model 8801 used to measure the surface temperature of the sample during the drying process. Accuracy ±0.1 °C.
(g) Hot wire anemometer with digital reading, brand INSTRUTEMP, model AMI 300 with a resolution of 0.01 m/s for measuring the air velocity inside the oven.
(h) Thermographic camera, brand FLI, model C5, for measuring the surface temperature of the sample, making it possible to verify possible temperature gradients on the surface of the sample during the drying process.

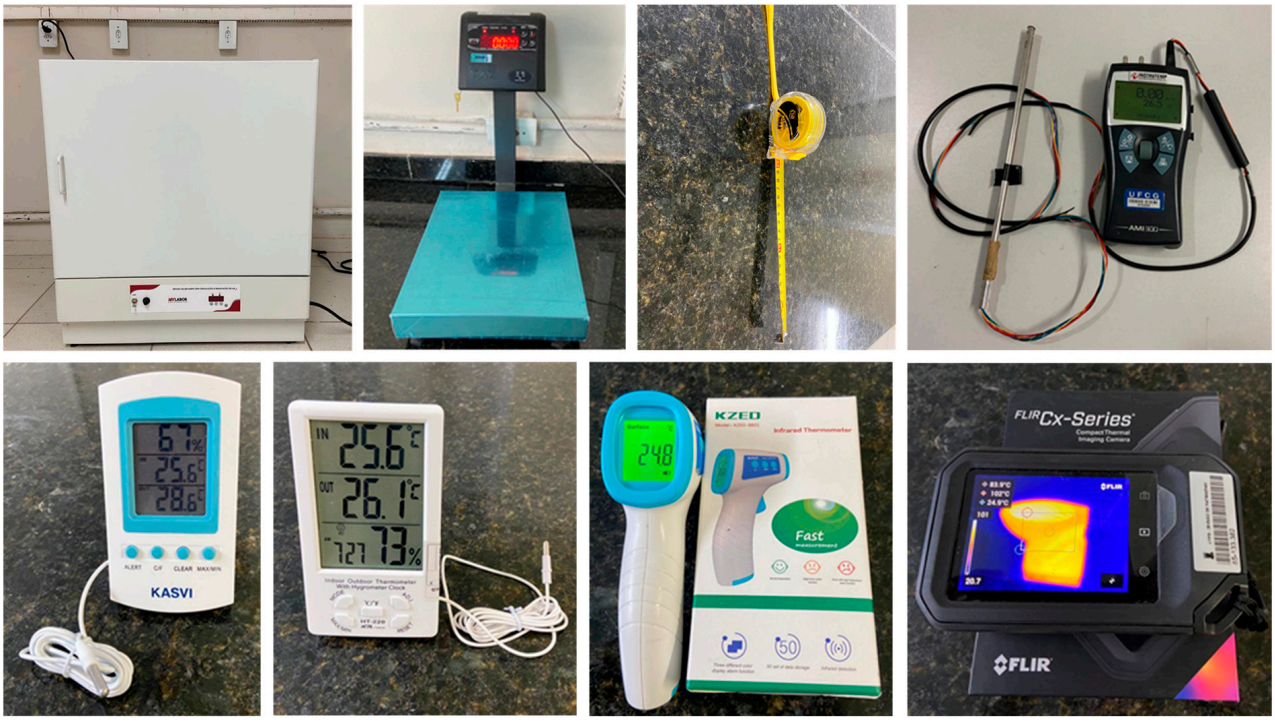

Figure 2. Equipment used in drying experiment: oven, digital scale, measuring tape, hot wire anemometer, two thermo-hygrometers, digital infrared thermometer and thermographic camera.

2.1.2. Experimental Procedures

The collection of each sample was carried out at the partner company approximately 2 h after the removal from their respective molds. It was considered important to wait this period of time so that the sanitary toilets acquired the necessary rigidity for future and constant handling during the oven drying experiments. The time between sample collection at the partner company and the beginning of each drying experiment at the laboratory placed in the University was approximately 30 min.

After the sample arrived at the laboratory, the first step was to measure the mass, surface temperature and main dimensions of the sanitary toilet, as well as the air tempera-

ture and relative humidity outside of the oven. The main dimensions of the sanitary toilet measured were the height, length and width of the upper part, and the length and width of the bottom part. The sanitary toilet was then taken inside the oven to carry out the drying experiment. For this stage, the air temperature inside the oven was set at the desired value for each experiment (30 °C or 40 °C) through the equipment's temperature controller.

At pre-defined intervals, the sanitary toilet was removed from the oven to carry out measurements of the surface temperature, mass and main dimensions. The surface temperature of the sample at each instant of time was defined as the average calculated from measurements at three previously established points, using a digital infrared thermometer. Each of the three points were located on the front, the side and the back of the sanitary toilet, as shown in Figure 3.

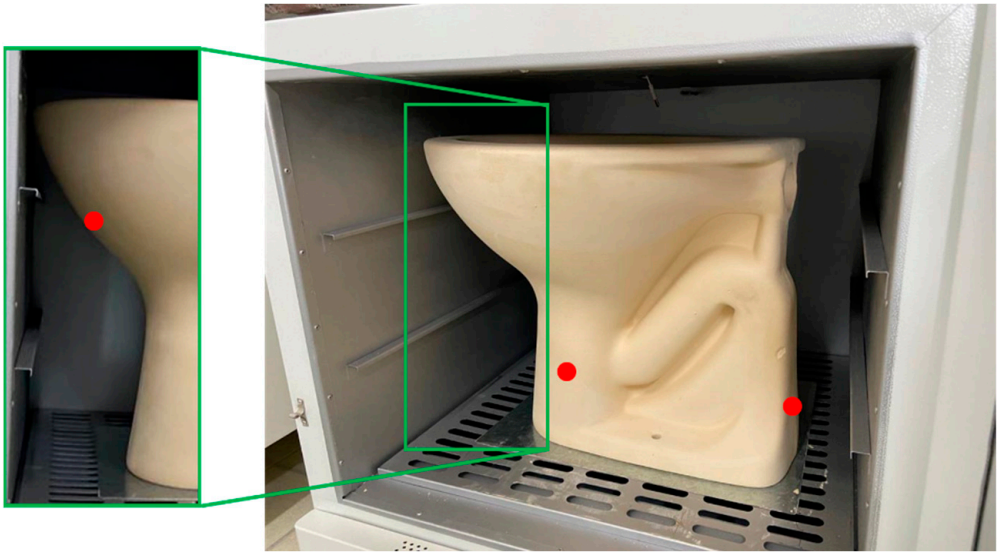

Figure 3. Indication of temperature measurement points at sample surface.

From the literature, it is well known that moisture loss rates are higher at the beginning of the drying process, regardless of the material, thus requiring data collection in shorter time intervals. As the process develops, the time interval can be increased. Thus, the measurements were performed at intervals of 10, 20 and 30 min, with six repetitions for each measurement. Next, 12 measurements were performed with an interval of 1 h each, followed by measurements every 2 h until the moment when the mass of the sample remained constant for 4 measurements in sequence. Immediately after this stage, the sample remained in the oven for another 24 h, at the same operating temperature, to obtain the equilibrium mass, and then for another 24 h at a temperature of 105 °C to obtain the dry mass of the sample. Such parameters are useful to calculate the moisture content of the sample as a function of the drying time. The described procedure was adapted from the works developed by Silva [35] and Silva [36], who experimentally studied the drying of industrial ceramic blocks and hollow ceramic bricks, respectively.

From the first drying experiment, it was verified that the absolute humidity in the interior and exterior regions of the oven were very close for the same instant of time. This outcome occurred due to a good renewal of the air inside the oven. Thus, for the other experiments, the indoor relative humidity was calculated instead of being measured experimentally. This methodology facilitates the performance of experiments and reduces the time for which the sample remains outside the oven. As the thermo-hygrometer used to measure the drying air conditions was positioned at the back of the oven (behind the part), it was only possible to read it after removing that part from the oven. It is important to note that this same methodology was used in several other experimental works on drying ceramic materials [35,36].

From the first experiment, it was also verified that the dimensional variations of the sample occur very slowly. Thus, the dimensional measurements of the sanitary toilets were carried out as follows: measurements taken one, three, six and twelve hours after the beginning of the experiment, followed by measurements at twelve-hour intervals. With the same periodicity, pictures of the samples were taken with a thermographic camera to verify the existence of temperature gradients on the surface of the piece.

2.1.3. Drying Experiment Locations

The drying experiments of the sanitary toilets were carried out in two different laboratories:

- Laboratory of Synthesis and Characterization of Thin Films (LABFILM), located in the Center for Alternative and Renewable Energy at the Federal University of Paraíba, João Pessoa, Brazil.
- New Materials Technology Laboratory (TECNOMAT), located in the Technology Center (Materials Engineering Department) at the Federal University of Paraíba, João Pessoa, Brazil.

The reason for carrying out the drying experiments in two different laboratories was due to the interest in evaluating the influence of air relative humidity, for the same air temperature, on the moisture removal during the drying process.

The LABFILM laboratory has two air conditioning units and a dehumidifier, which are turned on 24 h a day, the air temperature and relative humidity and, consequently, the absolute humidity of this environment are very low.

Although the TECNOMAT laboratory also had air conditioning devices, they were turned off during the experiments to avoid dehumidifying the ambient air. In addition, a door that gives access to the outside of the building was kept open during the experiments to ensure good ventilation and air renewal in the laboratory, and also to maintain high air relative humidity in the ambient area outside of the oven.

2.1.4. The Studied Cases

Table 1 presents the cases studied experimentally with their respective locations, types of ventilation, temperatures (T), relative humidities (RH) and average velocities (v) of the drying air, initial masses (m_0) and temperatures (θ_0) of the sanitary toilets.

Table 1. Cases studied experimentally.

Case	Local	Type of Ventilation	Drying Air			Sanitary Toilet	
			T (°C)	RH (%)	v (m/s)	m_0 (g)	θ_0 (°C)
1	LABFILM	Forced	30.1	23	0.1	16,370	26.0
2	LABFILM	Forced	40.0	14	0.1	18,120	25.0
3	TECNOMAT	Forced	30.0	51	0.1	15,890	24.8
4	TECNOMAT	Forced	40.0	35	0.1	15,980	25.1

The temperature and relative humidity values for the drying air presented in Table 1 represent the averages of the measurements that were carried out during the entire drying process at the pre-established time instants, as previously described. The temperature values of 30 and 40 °C were defined as they are usually the minimum and maximum limits of air temperature allowed in the pre-drying sector of the sanitary ware manufacturing process used in the ceramic industry.

All experiments were performed with forced convection and external air renewal. The drying air velocity value was obtained through averaging the values read at 8 different points inside the oven using a hot wire anemometer, at room temperature and with a sample inside.

2.2. Auxiliary Calculations

After carrying out the drying experiments, auxiliary calculations were developed to determine important parameters based on variations in the mass, dimensions and temperature of the samples throughout the process, as well as the air temperature and relative humidity. Such parameters are useful to compare and discuss the results for the different cases studied experimentally.

- Mass of water

The amount of water in the sanitary toilet (m_w), at each measurement time, was calculated as a function of the sample mass (m), at the time of interest, and the dry mass of the sample (m_d), as follows:

$$m_w = m - m_d. \tag{1}$$

As previously mentioned, the dry mass of the sample was the mass value obtained at the end of the drying process after it remained in the oven for 24 h at a temperature of 105 °C. It was considered that all residual water in the sample was evaporated after this process.

- Moisture content on a dry basis

The moisture content of the sample (M), at each measurement time, was calculated as a function of the water mass of the sample (m_w), at the time of interest, and the dry mass of the sample (m_d), as follows:

$$M = \frac{m_w}{m_d}. \tag{2}$$

- Drying rate

Drying rate was defined as the derivative of moisture content based on drying time. In this way, the drying rate of the sample at a given instant of time, i.e., $dM(t)/dt$, was calculated (approximately) as follows:

$$dM(t)/dt = -\frac{M(t) - M(t - \Delta t)}{\Delta t}, \tag{3}$$

where $M(t)$ is the moisture content at time t, $M(t - \Delta t)$ is the moisture content at old time $(t - \Delta t)$, and Δt is the time interval recorded between the two consecutive measurements. For convenience, the minus sign was introduced in the equation to obtain positive and decreasing values for the drying rate.

- Linear retraction of the sample

Since it is a complex geometry, it is very difficult to quantify the volumetric shrinkage of the sanitary toilets during the drying experiments. In contrast, five of the main dimensions of the sanitary toilet were measured during the drying experiments. The five measurements were height, length of the upper base, width of the upper base, length of the lower base and width of the lower base, as shown in Figure 4. The linear retraction of the sample at a given instant of time (t) was then defined as the average of these five measurements at that instant of time divided by the average of these five measurements at the beginning of the drying process ($t = t_0 = 0$ s), as follows:

$$\text{Linear retraction} = \frac{\sum_{i=1}^{5} L_i(t)}{\sum_{i=1}^{5} L_i(t_0)}, \tag{4}$$

where L_i is the measure value in the location i, which ranges from 1 to 5.

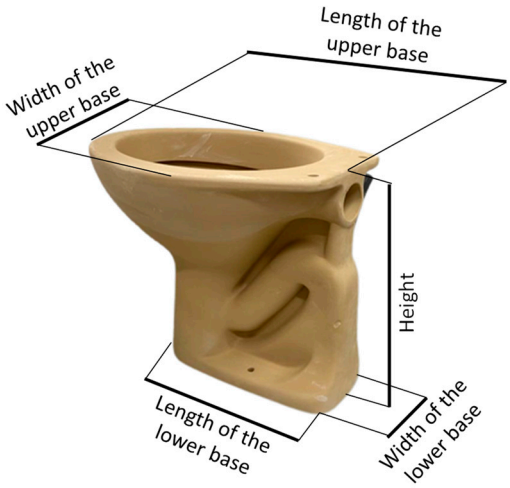

Figure 4. Main measurements of sanitary toilet used in linear retraction analysis.

- Relative humidity of the drying air

To calculate the relative humidity of the air inside the oven for each instant of time, the following methodology was used:

From the temperature (T) and relative humidity of the air (RH) outside the oven, which were obtained using a digital thermo-hygrometer, the saturation vapor pressure (P_g) was calculated using the Tetens equation [37], followed by the calculation of the vapor pressure (P_v):

$$P_g = 0.61078 \times e^{\left(\frac{17.27T}{T+237.3}\right)}, \quad (5)$$

$$P_v = RH \times P_g, \quad (6)$$

where P_g and P_v are given in kPa, RH is given in decimal value, and T is the temperature in Celsius degrees (°C).

Subsequently, the absolute humidity of the air (ω) outside the oven i, which was defined as the ratio between the mass of water vapor in the air (m_v) and the mass of dry air (m_A) s, was calculated as follows [38]:

$$\omega = \frac{m_v}{m_A} = \frac{M_v P_v \forall / \bar{R}T}{M_A P_A \forall / \bar{R}T} = \frac{M_v \times P_v}{M_A \times P_A} = \frac{M_v \times P_v}{M_A \times (P - P_v)} = 0.622 \frac{P_v}{(P - P_v)}, \quad (7)$$

where P = 101.325 kPa is the atmospheric pressure at sea level. The symbol $\forall$ represents the volume of the air mass and vapor.

Herein, it was considered that the absolute humidity inside the oven was equal to the absolute humidity outside the oven. As the atmospheric pressures were equal in the locations, the vapor pressures (P_v) in the two regions were also equal. Thus, the saturation vapor pressure (P_g) was calculated for the air temperature inside the oven using Equation (5).

Finally, knowing the vapor pressure (P_v) and the saturation vapor pressure (P_g), the relative humidity of the air inside the oven was calculated using Equation (6).

It was important to emphasize that Monteith and Unsworth [39] reported that the saturation vapor pressure values of the Tetens equation presented an error of up to 1 Pa when compared with exact values for temperatures up to 35 °C. To confirm reliability, different results of relative humidity inside the oven were compared for each of the experiments carried out, using the above-described methodology, with the exact results obtained using the Computer-Aided Thermodynamic Tables 3 (CATT3) software. Based on this analysis, it was found that the maximum absolute error obtained for the relative humidity inside the oven was 0.02%, guaranteeing the reliability of the Tetens equation in the temperature range studied (between 30 and 40 °C).

3. Results and Discussion

3.1. Drying Kinetics

Table 2 indicates the drying air conditions for each proposed case, as well as the initial mass (m_0), initial water mass (m_{w0}), equilibrium mass (m_e) and dry mass (m_d) of the samples. From the analysis of the Table 2, it is observed that the values of relative humidity of the drying air for the first two cases, which were carried out in LABFILM, are lower than the values obtained in the other cases, which were carried out in TECNOMAT. This outcome occurred because the LABFILM has a dehumidifier and two air conditioning units that remained on during the experiments, while the drying experiments at the TECNOMAT were carried out without a dehumidifier and with the air conditioning devices turned off.

Table 2. Initial, equilibrium and dry mass results for each experiment.

Case	Drying Air			Sanitary Toilet			
	T (°C)	RH (%)	v (m/s)	m_0 (g)	m_{w0} (g)	m_e (g)	m_d (g)
1	30.1	23	0.1	16,370	3040	13,400	13,330
2	40.0	14	0.1	18,120	3080	15,100	15,040
3	30.0	51	0.1	15,890	2865	13,110	13,025
4	40.0	35	0.1	15,980	2875	13,165	13,105

It is also observed that, for the same laboratory, the higher the temperature of the drying air, the lower the air relative humidity. This result is in line with expectations since the increase in temperature implies an increase in the saturation vapor pressure, increasing the capacity of the air to retain water in the vapor state (humidity).

From the analysis of Table 2, it is also noticed that even respecting the same time interval between the removal of the sample from the mold and the beginning of the drying experiment, there is a reasonable difference in the initial masses of the samples (m_0). In absolute terms, the maximum difference between the masses of the samples is 2230 g, comparing Cases 2 and 3. In percentage terms, the mass of sample 3 corresponds to 87.69% of the mass of sample 2. This outcome could have occurred for three main reasons: dimensional differences in the molds of the parts, the time the samples remained in the molds and differences in the composition of the slip (raw material) in each of the samples, given that the collections were carried out in different weeks. The average initial mass of the samples in the four experiments and the respective standard deviation was 16,590 $\pm$ 902 g.

Figure 5 shows the comparison between the average moisture content of the samples as a function of time for all the experiments. Such results are important to understand the drying kinetics of sanitary toilets for different conditions of air temperature and relative humidity.

From the analysis of Figure 5, it is observed that drying occurred more quickly for the experiment with higher temperature (40 °C) and lower relative humidity (14%) of the drying air (Case 2), i.e., the moisture content reduced from its initial value to the equilibrium value in a shorter time. The case with the second fastest drying was that carried out in the TECNOMAT (highest relative humidity) with a temperature of 40 °C (Case 4). Next, there are Cases 1 (T = 30.1 °C; RH = 23%) and 3 (T = 30 °C; RH = 51%).

These results show that the drying air temperature is not the only factor that influences the drying kinetics. The air relative humidity is a parameter of fundamental importance in the drying of ceramic materials. The reduction in relative humidity favors the mass transfer of water from the interior of the piece to the drying air as a result of the higher water evaporation rate on the surface.

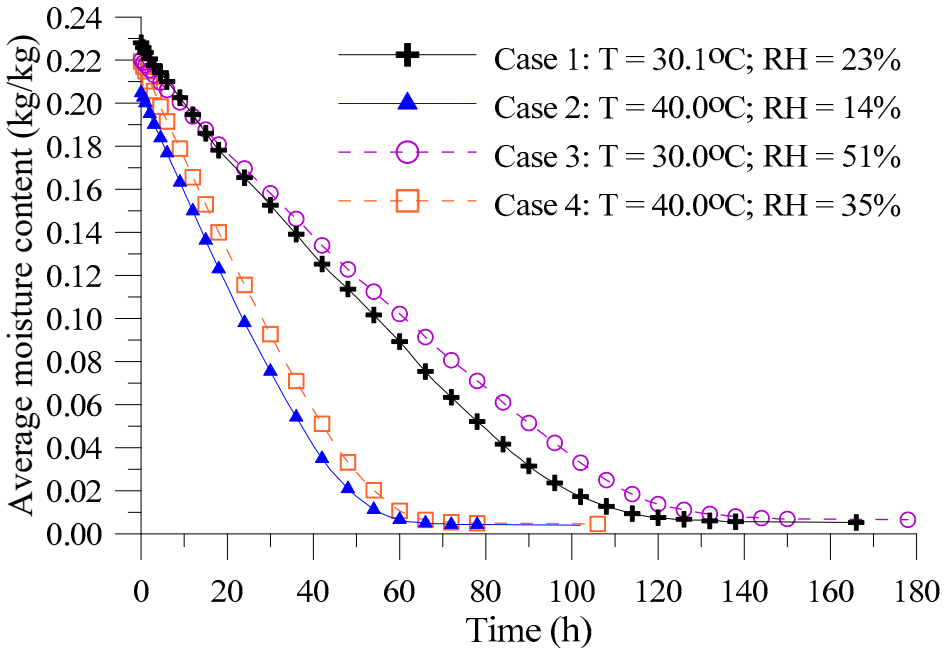

Figure 5. Average moisture content of samples as a function of time for all analyzed cases.

Analyzing the average moisture content curves as a function of time for each of the analyzed cases, there is a feeling of a linear relationship between the two variables in the initial moments of the process, which would indicate the first drying stage, in which the water evaporation rate from the product does not change with time. However, when analyzing the drying rate curves as a function of time (Figure 6), it is observed that the drying rate is already decreasing with time in the initial moments of the process, although more accentuated decays are observed, in general, in the second half of the drying experiment. In the final moments of the drying process, a curvilinear decay of the drying rate as a function of time is observed, tending to zero when approaching the hygroscopic equilibrium condition.

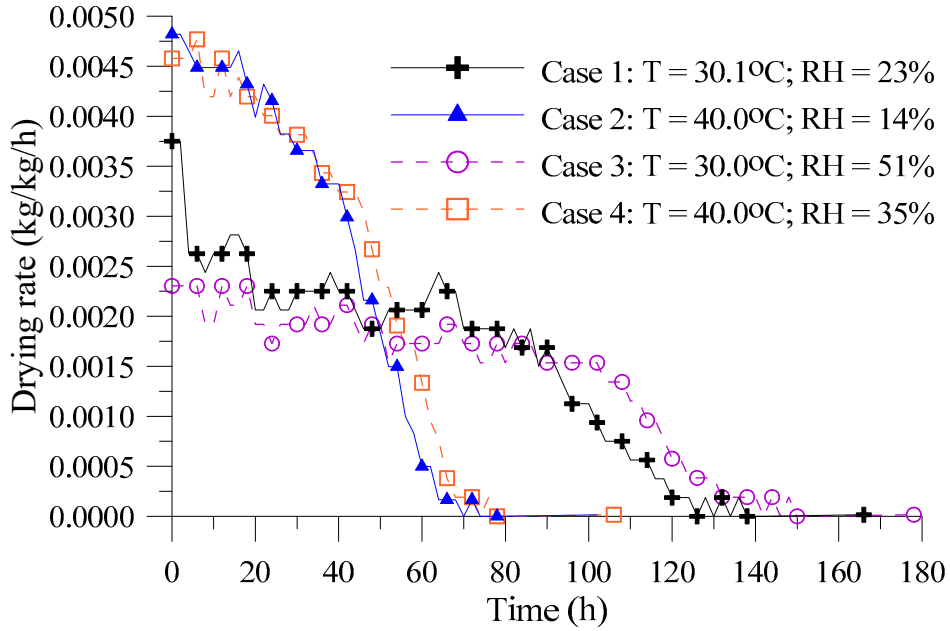

Figure 6. Drying rate of samples as a function of time during drying process.

The lack of a constant drying rate period was also reported in the literature for drying ceramic bricks [8,36], industrial ceramic blocks [5,35] and sisal fiber [40] with drying air temperatures varying between 50 and 100 °C. However, for such cases, the most accentuated decay of the drying rate with time occurred in the initial moments of the process. Reasons for this outcome are the lower values of initial moisture content of the samples and the higher values for drying air temperature, material composition, volumetric shrinkage behavior and part geometry, which are all factors that influence the effective mass diffusivity of the product.

Analyzing Figure 6, we observe the proximity between the drying rates for Cases 2 and 4 during practically the entire process. Cases 1 and 3 also show similar drying rates during most of the process.

Figure 7 illustrates the comparison between the drying rates of the samples as a function of the average moisture content for all analyzed cases. It is noticed that, for all experiments, there is a more accentuated decay in the drying rate when the average moisture content of the sample approaches to 0.03 kg/kg.

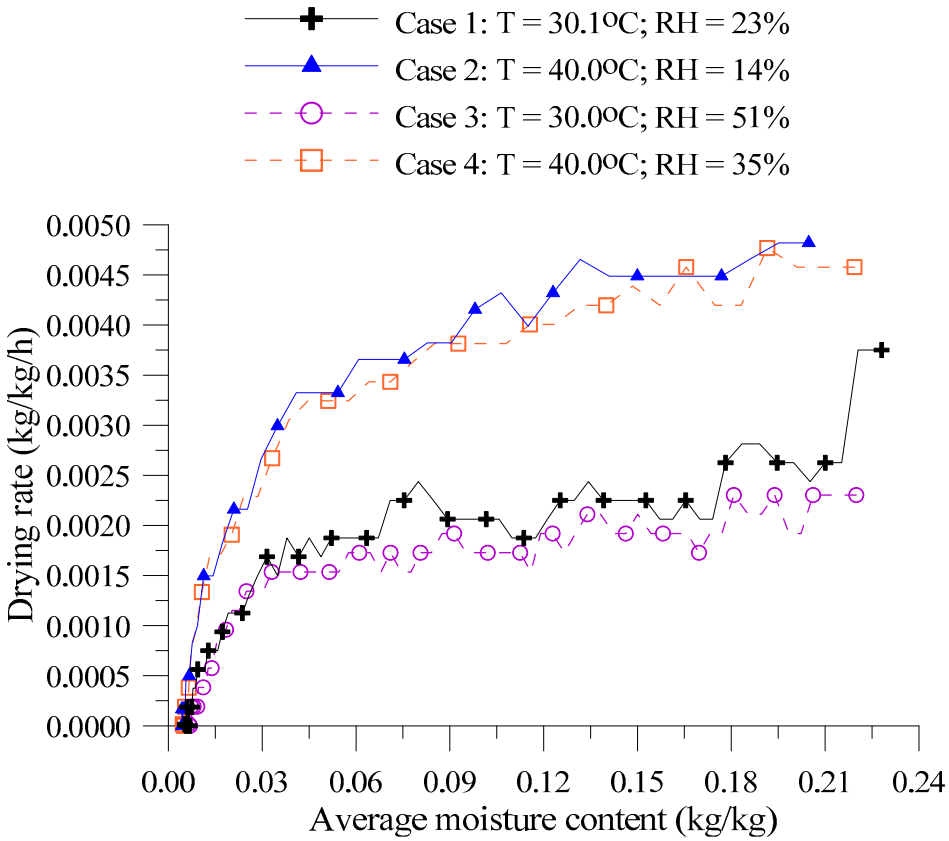

Figure 7. Drying rate as a function of average moisture content of samples during drying process.

Figure 8 show images of the sample used in Case 3 at the beginning and end of the drying process. It is possible to observe a change in the color of the piece due to the loss of moisture and heating during the experiment. However, no cracks or fissures were observed as a result of the drying process. This result is in line with expectations, as these defects only occur when temperature gradients and moisture content in the part are high; for ceramic materials, the tendency is for this to happen at higher drying air temperatures and lower air relative humidity. These results corroborate those obtained by Silva [36], who only observed small cracks in hollow ceramic bricks for temperatures above 80 °C, and Silva [35], who reported small cracks in industrial hollow ceramic blocks for temperatures above 60 °C.

(**a**) (**b**)

Figure 8. Sample used in Case 3 (TECNOMAT laboratory; T = 30.0 °C; RH = 51%) before (**a**) and after (**b**) oven drying experiment.

3.2. Heating Kinetics

From Figure 9, which illustrates the surface temperature of the sample as a function of time, it can be seen that, for all the cases analyzed, the surface temperature of the sample increases rapidly from its initial value to an intermediate value, while between the initial temperature and the drying air temperature, it remains oscillating at this intermediate value for a good part of the experiment; only at the end of the process does its value approach the temperature of the drying air, i.e., the thermal equilibrium condition.

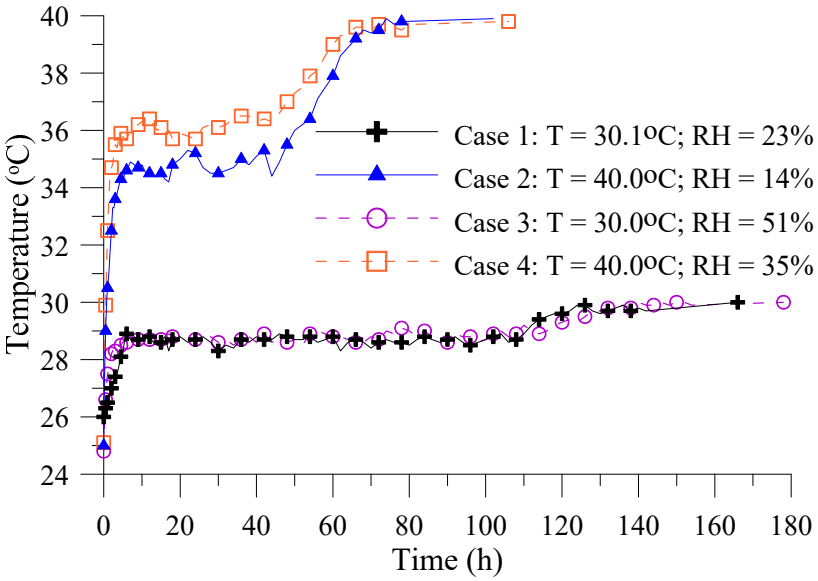

Figure 9. Surface temperature of samples as a function of time during drying process.

From observations made during the experiments, it was noticed that the surface temperature increased again at the moment when the change in the color of the sample became more evident, which was already in the final stage of the drying process. Thus, it is reasonable to assume that the change in sample color modified the emissivity of the material, which was a variable that directly influenced the temperature read using the digital infrared thermometer. Moreover, at this drying moment, the sample was almost dried and the energy absorbed by it was used almost in totality as sensible heat to increase its temperature.

The sharp increase in the surface temperature of the samples in the initial moments of the drying processes is a characteristic of the first falling-rate period, being one more indication that, in the experiments carried out, there was no first stage of drying. The constant drying-rate period occurs at constant temperature with values equal to the wet bulb temperature of the drying air.

Among the experiments carried out at 40 °C, it can be seen that the intermediate temperature at which its value oscillated was higher for the case with higher relative humidity (Case 4). In addition, it is observed that both the cases reached the upper temperature level at approximately the same instant of time. The experiments carried out with a temperature of 30 °C showed very similar behavior throughout the entire experiment, both in terms of the intermediate temperature value and in the instant when the upper temperature level was reached.

Figure 10 shows the comparison between the surface temperatures of the samples as a function of the average moisture content for all analyzed cases. Once again, it is evident that the surface temperature of the sample increases rapidly from its initial value to an intermediate value, with a small variation in the average moisture content, and remains at this level until the average moisture content reaches a value close to 0.03 kg/kg. From this drying moment, the temperature increases again, approaching the temperature of the drying air.

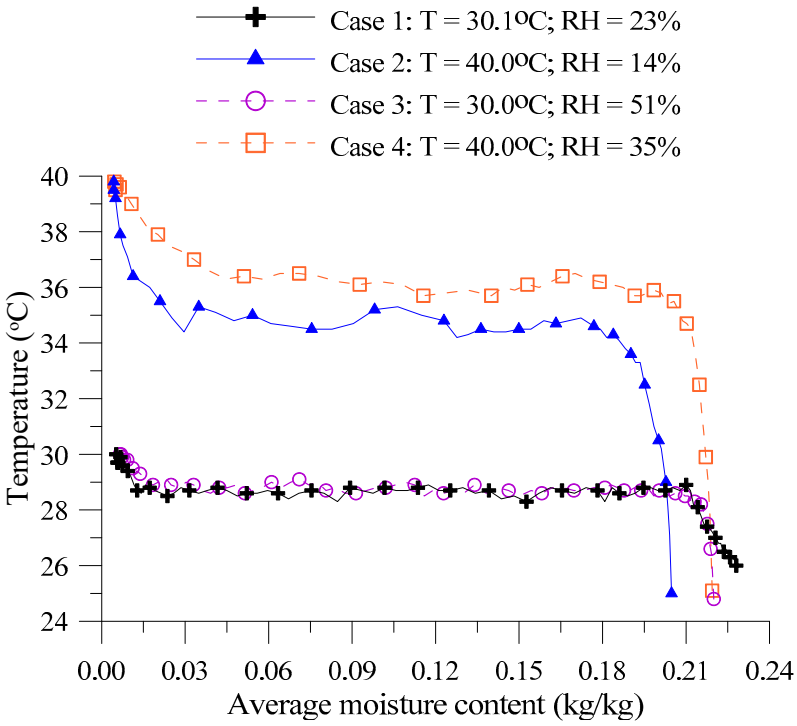

Figure 10. Surface temperature of sample as a function of average moisture content.

Figure 11 shows the thermograms obtained in two instants of time for Case 3 (LAB-FILM; T = 30.0 °C; RH = 51%). The first time instant was at the intermediate temperature level (t = 36 h), while the second time instant was at equilibrium condition (t = t_e = 178 h). In the thermogram, it is possible to identify the temperature variations in different points of the parts. From the analysis of the Figure 11, it can be noticed that the temperatures obtained are slightly below the values presented previously for surface temperature. This result occurred because the measurements used to create the graphs of surface temperature versus time were taken using a digital infrared thermometer when the sample was inside the oven, while the images shown in Figure 11 were obtained from a thermographic camera with the sanitary toilet in the digital scale for weighing. In the time interval between removing the toilet from the oven, placing it on the scale, closing the oven door and writing

down the mass before taking the photo, there is a heat transfer from the sample to the environment, reducing its temperature.

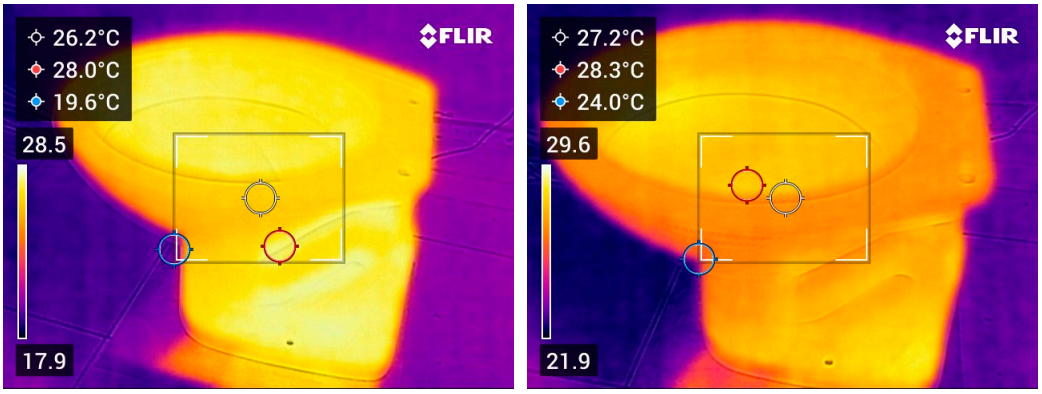

(**a**) (**b**)

Figure 11. Thermograms of sample used in Case 3 (T = 30.0 °C and RH = 51%) for time instants (**a**) t = 36 h and (**b**) t = t_e = 178 h.

Table 3 indicates the initial moisture content (M_0), the equilibrium moisture content (M_e), the time needed to reach the equilibrium condition (t_e) and the equilibrium surface temperature (θ_e) for each of the experiments. It is observed that despite the identical time interval between removing the sample from the mold and the beginning of the drying experiment, which was approximately two and a half hours, there is a reasonable difference in the initial moisture content of the samples.

Table 3. Results of initial and equilibrium moisture content, final temperature and time to reach higroscopic equilibrium.

Case	Drying Air			Sanitary Toilet			
	T (°C)	RH (%)	v (m/s)	M_0 (kg/kg, d.b)	M_e (kg/kg, d.b)	t_e (h)	θ_e (°C)
1	30.1	23	0.1	0.22806	0.00525	166	30.0
2	40.0	14	0.1	0.20479	0.00399	102	39.9
3	30.0	51	0.1	0.21996	0.00653	178	30.0
4	40.0	35	0.1	0.21938	0.00458	106	39.8

The highest initial moisture content was observed for the sample used in Case 1, with a value of 0.22806, while the lowest value was observed for Case 2, with a value of 0.20479; this variation represents a difference of 0.02327 in absolute terms and 11.20% in percentage terms. Comparing these results with the results presented in Table 2, it is noticed that higher values of initial moisture content are not associated with higher values of initial mass.

The reasons for the different values obtained for the initial moisture content are the possible different air conditions in the casting sector of the partner company during the steps of filling the mold, draining the excess slip and removing the parts from the mold; the rest period of the part in the mold; and mold moisture absorption efficiency. The final factor, according to Cavalcante [4], tends to decrease with the increase in cycle counts.

Upon examining Table 3, it is evident that the higher the temperature inside the oven, the shorter the time needed to reach the equilibrium condition (t_e), and that, for two experiments carried out at the same temperature, the time was shorter for lower values of relative humidity. In this way, the ascending order of the total drying time for the experiments was 2-4-1-3.

It is observed that the difference between the total drying time for the experiments carried out at a temperature of 40 °C was only four hours. As for the experiments carried out with a temperature of 30 °C, the difference in the total drying time was 12 h. This result indicates that relative humidity has a greater influence on the total drying time for

a temperature of 30 °C. Such differences in the values of the total drying time, identified between experiments carried out at the same temperature, would be greater if the values of initial moisture content (M_0) were closer.

It can be seen that the ascending order of the equilibrium moisture content (M_e), i.e., 2-4-1-3, was equal to the ascending order of the time to reach the equilibrium condition (t_e), i.e., the higher the drying air temperature, the lower the value of M_e, and for the same temperature, the lower the relative humidity, the lower the value of M_e.

Table 4 indicates the time interval required to reduce the moisture content from 0.20 to 0.15 ($\Delta t_{M = 0.20 \rightarrow 0.15}$), from 0.20 to 0.10 ($\Delta t_{M = 0.20 \rightarrow 0.10}$), from 0.20 to 0.05 ($\Delta t_{M = 0.20 \rightarrow 0.05}$) and from 0.20 to 0.01 ($\Delta t_{M = 0.20 \rightarrow 0.01}$). Normally, companies in the sanitary ware sector define a fixed time, based on experience, for which each type of product must remain in the pre-drying sector before moving to the drying stage. Usually, this time varies from one to three days, depending on the type of product [41]. A better way to manage this process would be to define the ideal moisture content in which the product should be dried at a high temperature, for example, when its value is equal to 0.15. Based on the desired moisture content and the air conditions in the environment where the drying at low temperatures is being carried out, it is possible to estimate how long the product should remain in the pre-drying sector before being transferred to drying at high temperatures.

Table 4. Comparison between times needed to reduce average moisture content of sample from 20 to 15, 10, 5 and 1% in dry basis.

Case	Drying Air			Sanitary Toilet			
	T (°C)	RH (%)	v (m/s)	$\Delta t_{M = 0.20 \rightarrow 0.15}$ (h)	$\Delta t_{M = 0.20 \rightarrow 0.10}$ (h)	$\Delta t_{M = 0.20 \rightarrow 0.05}$ (h)	$\Delta t_{M = 0.20 \rightarrow 0.01}$ (h)
1	30.1	23	0.1	21.212	44.829	69.295	102.922
2	40.0	14	0.1	10.958	22.509	36.233	54.280
3	30.0	51	0.1	24.850	52.022	81.738	119.750
4	40.0	35	0.1	11.454	23.890	38.147	56.516

In this way, it is possible to adapt the pre-drying time of the product depending on the air conditions in the environment, which can vary significantly at different times of the year, to verify if there is poor control of the process parameters. In addition, this methodology serves as a decision-making tool to obtain a shorter operating time in the pre-drying sector, providing a reduction in energy consumption.

The same ascending order that was observed for the total drying time can also be observed for the time intervals required to reduce the average moisture content from 0.20 to 0.15, 0.10, 0.05 and 0.01, i.e., Cases 2-4-1-3. In this way, the higher the temperature inside the oven, the shorter the time intervals required to reduce the average moisture content from 0.20 to 0.15, 0.10, 0.05 and 0.01, while for two experiments carried out at the same temperature, the time intervals are shorter for lower values of air relative humidity.

Comparing the time intervals for experiments carried out at the same temperature, it is noticed that there is a greater proximity between the cases carried out at 40 °C than the cases carried out at 30 °C, as well as between the varied total drying times (t_e).

3.3. Linear Retraction Kinetics

Table 5 presents the results of final linear retraction and final mass variation for all drying experiments. The lower the value of the final linear retraction, the greater the shrinkage of the part during the drying experiment. It is observed that the greatest shrinkages are associated with the greatest mass variations, which occurred for Cases 1 and 2.

Figure 12 shows a comparison between the linear retraction of the samples as a function of time for all analyzed cases. It is observed that the higher the air temperature, the greater the slopes of the linear retraction curve as a function of time. Furthermore, for the same temperature, the lower the air relative humidity, the greater the slopes of the linear retraction curve as a function of time.

Table 5. Results of final linear retraction and final mass variation for all drying experiments.

Case	Drying Air			Final Linear Retraction (-)	Final Mass Variation (g)
	T (°C)	RW (%)	v (m/s)		
1	30.1	23	0.1	0.97120	3040
2	40.0	14	0.1	0.97201	3080
3	30.0	51	0.1	0.97387	2865
4	40.0	35	0.1	0.97391	2875

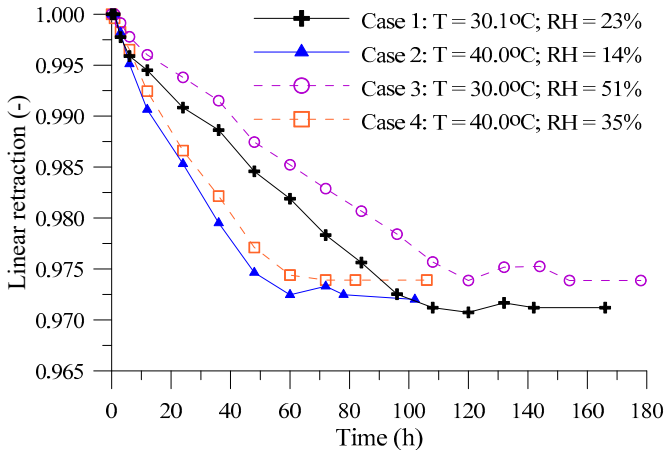

Figure 12. Linear retraction of sample as a function of time during drying process.

In general, greater slopes in linear retraction curves as a function of time imply greater chances of defect formation. For this reason, greater care must be taken in the initial moments of the drying process, especially when this process is carried out at high temperatures and low relative humidities. For such situations, it is advisable that the temperature of the drying air is gradually raised in the initial moments of the process, ensuring that the phenomenon of shrinkage is controlled at this most problematic stage.

Figure 13 illustrates the linear retraction as a function of the average moisture content of the sample for all cases. From the analysis of this figure, it is possible to observe that there is an almost linear relationship between the two variables for all the experiments. As the average moisture content of the sample decreased during the experiment for all analyzed cases, the linear retraction variable also decreased its value, which, in turn, indicated greater shrinkage in the part. There is also a great proximity between the curves obtained for each case.

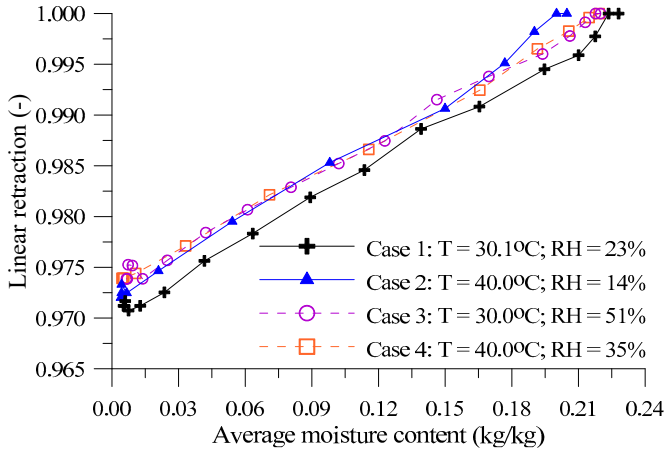

Figure 13. Linear retraction of sample as a function of average moisture content during drying process.

4. Conclusions

In this research, the engineering problem related to drying of sanitary ware in an oven at low temperatures was studied, and the effect of the main drying parameters (temperature and relative humidity) were evaluated. Based on the results obtained, it can be concluded that:

(a) The increase in air temperature and reduction in air relative humidity resulted in faster drying and heating.
(b) The drying of sanitary ware occurred in the falling drying rate period.
(c) The experiment carried out with the highest temperature and lowest relative humidity (Case 2: T = 40.0 °C; RH = 14%) presented the fastest drying rate among all the analyzed cases.
(d) The study proved that, for certain physical situations, it is more interesting to dedicate efforts to reduce the relative humidity of the drying air instead of looking for solutions to increase its temperature.
(e) No cracks or fissures were observed in the sanitary toilets as a result of the drying process at low temperatures ranging from 30 to 40 °C.
(f) There is a correlation between the linear retraction and moisture content of the sample; thus, the greater the moisture loss, the greater the sample shrinkage for each drying experiment.
(g) The higher the air temperature and the lower the air relative humidity, the greater the slope of linear retraction curves along the drying process.

Finally, this work is expected to contribute to a better understanding of the drying process of ceramic materials, and provide support for engineers, specialists, academics and industrialists in making decisions to optimize the drying process. The aim is to increase the quality of the product and reduce the processing time, energy consumption and environmental impacts. In this way, it will be possible to lead companies in the ceramic sector on a path that will make them more competitive in national and international markets.

Author Contributions: Conceptualization, R.S.G., K.C.G., J.M.A.M.G., L.B.A. and B.T.A.S.; methodology, R.S.G., L.B.A., H.L.F.M. and D.B.T.V.; validation, R.A.Q., G.C.P.S., A.S.O. and A.F.V.; formal analysis, R.S.G., K.C.G., J.M.A.M.G. and G.R.F.B.; writing—original draft preparation, R.S.G., K.C.G., D.B.T.V. and A.G.B.L.; writing—review and editing, H.L.F.M., R.A.Q., G.C.P.S. and A.S.O.; supervision, K.C.G., J.M.A.M.G. and L.B.A.; funding acquisition, K.C.G., J.M.A.M.G. and A.G.B.L. All authors have read and agreed to the published version of the manuscript.

Funding: This research was funded by CNPq (Grant numbers 443863/2018-0, 148893/2019-8 and 308255/2022-4) and FAPESQ-PB/CAPES (Grant number 18/2020) (Brazilian research agencies).

Data Availability Statement: The data that support the findings of this study are available upon request from the authors.

Acknowledgments: The authors are grateful to CNPq, CAPES, FINEP and FAPESQ-PB for the financial support, the DEXCO S.A (João Pessoa, Brazil), for the partnership and availability of samples, and the LABFILM and TECNOMAT laboratories at UFPB (João Pessoa, Brazil) and the Thermal and Fluid Computational Laboratory at UFCG (Campina Grande, Brazil) for research infrastructure.

Conflicts of Interest: The authors declare no conflict of interest.

Abbreviations

CATT3	Computer-Aided Thermodynamic Tables 3 software	[-]
$dM(t)/dt$	Drying rate	[kg/kg/s]
LABFILM	Laboratory of Synthesis and Characterization of Thin Films	[-]
L_i	Value of measurement i for calculating the linear retraction of the sample	[m]

m	Sample mass	[kg]
m_0	Initial mass of the sample	[kg]
m_A	Mass of dry air	[kg]
m_d	Dry mass of the sample	[kg]
m_e	Equilibrium mass of the sample	[kg]
m_v	Mass of water vapor in the air	[kg]
m_w	Water mass of the sample	[kg]
m_{w0}	Initial water mass of the sample	[kg]
M	Moisture content on a dry basis	[kg/kg]
M_A	Molecular mass of dry air	[kg/kmol]
M_0	Initial moisture content	[kg/kg]
M_e	Equilibrium moisture content	[kg/kg]
M_v	Molecular mass of water	[kg/kmol]
P	Atmospheric pressure at sea level	[Pa]
P_A	Partial pressure of dry air	[Pa]
P_g	Saturation vapor pressure	[Pa]
P_v	Vapor pressure	[Pa]
RH	Relative humidity	[decimal]
TECNOMAT	New Materials Technology Laboratory	[-]
t	Instant of time	[s]
t_0	Initial instant of time	[s]
t_e	Time to reach the equilibrium condition	[s]
T	Drying air temperature	[°C]
v	Velocity	[m/s]
Δt	Time interval between two consecutive measurements	[s]
$\Delta t_{M = 0.20 \rightarrow 0.15}$	Time required to reduce the moisture content from 0.20 to 0.15	[s]
$\Delta t_{M = 0.20 \rightarrow 0.10}$	Time required to reduce the moisture content from 0.20 to 0.10	[s]
$\Delta t_{M = 0.20 \rightarrow 0.05}$	Time required to reduce the moisture content from 0.20 to 0.05	[s]
$\Delta t_{M = 0.20 \rightarrow 0.01}$	Time required to reduce the moisture content from 0.20 to 0.01	[s]
θ	Temperature of the sample	[°C]
θ_0	Initial temperature of the sample	[°C]
θ_e	Equilibrium surface temperature	[°C]
$\forall$	Volume of the air	[m^3]
ω	Absolute humidity of the air	[kg/kg]

References

1. Santos, R.S. Study of the Drying Process of Structural Ceramic Blocks: Modeling and Simulation. Ph.D Thesis, Process Engineering, Federal University of Campina Grande, Campina Grande, Brazil, 2019. Available online: http://dspace.sti.ufcg.edu.br:8080/jspui/handle/riufcg/10549 (accessed on 20 November 2022). (In Portuguese).
2. ANICER—National Ceramic Industry Association—Sector Data. 2021. Available online: https://www.anicer.com.br/anicer/setor/ (accessed on 5 November 2022). (In Portuguese).
3. Lima, A.G.B.; Delgado, J.; Nascimento, L.P.C.; Lima, E.S.; Oliveira, V.A.B.; Silva, A.M.V.; Silva, J.V. Clay Ceramic Materials: From Fundamentals and Manufacturing to Drying Process Predictions. In *Transport Processes and Separation Technologies*, 1st ed.; Delgado, J.M.P.Q., Lima, A.G.B., Eds.; Springer: Cham, Switzerland, 2021; Volume 133, pp. 1–29.
4. Cavalcante, W.F.V. Use of Ceramic Waste from the Sanitary Ware Industry to Produce Pastes for Ceramic Coating. Master's Thesis, Mechanical Engineering, Federal University of Pernambuco, Recife, Brazil, 2005. Available online: https://repositorio.ufpe.br/handle/123456789/5394 (accessed on 24 November 2022). (In Portuguese).
5. Silva, A.M.V.; Delgado, J.; Guimarães, A.S.; Lima, W.M.P.B.; Gomez, R.S.; Farias, R.P.; Lima, E.; Lima, A.G.B. Industrial Ceramic Blocks for Buildings: Clay Characterization and Drying Experimental Study. *Energies* **2020**, *13*, 2834. [CrossRef]
6. Gomez, R.S.; Porto, T.; Magalhães, H.L.F.; Guedes, C.A.L.; Lima, E.S.; Wanderley, D.; Lima, A.G.B. Transient Thermal Analysis in an Intermittent Ceramic Kiln with Thermal Insulation: A Theoretical Approach. *Adv. Mater. Sci. Eng.* **2020**, *2020*, 6476723. [CrossRef]
7. Silva, J.B.; Almeida, G.S.; Lima, W.C.P.B.; Neves, G.A.; Lima, A.G.B. Heat and mass diffusion including shrinkage and hygrothermal stress during drying of holed ceramics bricks. *Defect Diffus. Forum* **2011**, *312*, 971–976. [CrossRef]
8. Silva, J.B.; Almeida, G.S.; Neves, G.A.; Lima, W.C.P.B.; Farias Neto, S.R.; Lima, A.G.B. Heat and mass transfer and volume variations during drying of industrial ceramic bricks: An experimental investigation. *Defect Diffus. Forum* **2012**, *326*, 267–272. [CrossRef]

9. Silva, V.S.; Delgado, J.; Lima, W.M.P.B.; Lima, A.G.B. Heat and mass transfer in holed ceramic material using lumped model. *Diffus. Found.* **2016**, *7*, 30–52. [CrossRef]
10. Zaccaron, A.; Dal Bó, M.; Peterson, M.; Nandi, V.S.; Montedo, O.R.K.; Angioletto, E.; Bernadin, A.M. Study of drying properties about heavy clay ceramics: A review. In Proceedings of the 63° Brazilian Congress of Ceramics, Bonito, Brazil, 4–7 August 2019. Available online: https://www.academia.edu/42766811/Estudo_das_propriedades_de_secagem_de_ceramica_vermelha_uma_revisao (accessed on 30 November 2022). (In Portuguese)
11. Zaccaron, A.; Nandi, V.S.; Bernardin, A.M. Fast drying for the manufacturing of clay ceramics using natural clays. *J. Build. Eng.* **2021**, *33*, 101877. [CrossRef]
12. Batista, V.R.; Nascimento, J.J.S.; Lima, A.G.B. Drying and volumetric retraction of solid and hollow ceramic bricks: A theoretical and experimental investigation. *Matér. Rio Jan.* **2009**, *14*, 1088–1100. [CrossRef]
13. Almeida, G.S.; Fernandes, M.A.F.; Fernandes, J.N.; Neves, G.A.; Barbosa de Lima, W.M.P.; Lima, A.G.B. Drying of industrial ceramic bricks: An experimental investigation in oven. *Defect Diffus. Forum* **2014**, *353*, 116–120. [CrossRef]
14. Mezquita, A.; Monfort, E.; Zaera, V. Ceramic tiles manufacturing and emission trading scheme: Reduction of co (2) emissions, european benchmarking. *Bol. Soc. Esp. Ceram. Vidr.* **2009**, *48*, 211–222.
15. Mezquita, A.; Boix, J.; Monfort, E.; Mallol, G. Energy saving in ceramic tile kilns: Cooling gas heat recovery. *Appl. Therm. Eng.* **2014**, *65*, 102–110. [CrossRef]
16. Kočí, V.; Scheinherrová, L.; Maděra, J.; Keppert, M.; Suchorab, Z.; Łagód, G.; Černý, R. Experimental and computational study of thermal processes in red clays exposed to high temperatures. *Energies* **2020**, *13*, 2211. [CrossRef]
17. Silvestri, L.; Forcina, A.; Silvestri, C.; Ioppolo, G. Life cycle assessment of sanitaryware production: A case study in Italy. *J. Clean. Prod.* **2020**, *251*, 119708. [CrossRef]
18. Cabral, M., Jr.; Azevedo, P.B.M.; Cuchierato, G.; Motta, J.F.M. Strategic Study of the Productive Chain of the Ceramic Industry in the State of São Paulo: Part III—Industries of Coloring, Sanitary Ware, and Technical Ceramics—Insulators. *Cerâm. Ind.* **2019**, *24*, 15–26. [CrossRef]
19. Almeida, G.S.; Silva, J.B.; Silva, C.J.; Swarnakar, R.; Neves, G.A.; Lima, A.G.B. Heat and mass transport in an industrial tunnel dryer: Modeling and simulation applied to hollow bricks. *Appl. Therm. Eng.* **2013**, *55*, 78–86. [CrossRef]
20. Almeida, G.S.; Tavares, F.V.S.; Lima, W.; Lima, A.G.B. Energetic and exergetic analysis of the clay bricks drying in an industrial tunnel dryer. *Defect Diffus. Forum* **2016**, *369*, 104–109. [CrossRef]
21. Martines-Lopez, E.; Lira-Cortes, L. Moisture transfer analysis during drying of brick by temperature and relative humidity profiles. *Eur. Sci. J.* **2013**, *9*, 109–122.
22. Tavares, F.; Neto, S.; Barbosa, E.; Lima, A.; Silva, C. Drying of ceramic hollow bricks in an industrial tunnel dryer: A finite volume analysis. *Int. J. Multiphys.* **2014**, *8*, 297–312. [CrossRef]
23. Khalili, K.; Bagherian, M.; Khisheh, S. Numerical simulation of drying ceramic using finite element and machine vision. *Procedia Technol.* **2014**, *12*, 388–393. [CrossRef]
24. Araújo, M.V.; Delgado, J.M.P.Q.; Lima, A.G.B. On the Use of CFD in Thermal Analysis of Industrial Hollow Ceramic Brick. *Diffus. Found.* **2017**, *10*, 70–82. [CrossRef]
25. Araújo, M.V.; Santos, R.S.; Silva, R.M.; Lima, A.G.B. Drying of Industrial Hollow Ceramic Brick: Analysis of the Moisture Content and Temperature Parameters. *Defect Diff. Forum* **2017**, *380*, 72–78. [CrossRef]
26. Araújo, M.V.; Pereira, A.S.; Oliveira, J.L.; Brandão, V.A.A.; Brasileiro Filho, F.A.; Silva, R.M.; Lima, A.G.B. Industrial ceramic brick drying in oven by CFD. *Materials* **2019**, *12*, 1612. [CrossRef] [PubMed]
27. Araújo, M.V.; Santos, R.S.; Silva, R.M.; Nascimento, J.B.; Santos, W.R.G.; Lima, A.G.B. Drying of industrial hollow ceramic brick: A numerical analysis using CFD. *Defect Diff. Forum* **2019**, *391*, 48–53. [CrossRef]
28. Araújo, M.V.; Correia, B.R.B.; Brandão, V.A.A.; Oliveira, I.R.; Santos, R.S.; Oliveira Neto, G.L.; Silva, L.P.L.; Lima, A.G.B. Convective drying of ceramic bricks by CFD: Transport phenomena and process parameters analysis. *Energies* **2020**, *13*, 2073. [CrossRef]
29. Araújo, M.V.; Sousa, A.C.; Luiz, M.R.; Cabral, A.S.; Pessoa, T.R.B.; Martins, P.C.; Silva, A.M.V.; Santos, R.S.; Oliveira, V.A.B.; Lima, A.G.B. Computational Fluid Dynamics Studies in the Drying of Industrial Clay Brick: The Effect of the Airflow Direction. *Diffus. Found. Mater. Appl.* **2022**, *30*, 69–84. [CrossRef]
30. Santos, R.S.; Peña, D.P.A.; Diniz, D.D.S.; Costa, G.A.; Queiroz, J.G.A.; Neto, S.R.F. Brick Drying Simulations by Finite Volume Method. *Mater. Sci. Forum* **2018**, *930*, 115–119. [CrossRef]
31. Santos, R.S.; Farias Neto, S.R.; Barbosa de Lima, A.G.; Silva Júnior, J.B.; Silva, A.M.V. Drying of ceramic bricks: Thermal and mass analysis via CFD. *Diffus. Found.* **2020**, *25*, 133–153. [CrossRef]
32. Lima, E.S.; Lima, W.M.P.B.; Silva, S.K.B.M.; Magalhães, H.L.F.; Nascimento, L.P.C.; Gomez, R.S.; Porto, T.R.N.; Lima, A.G.B. Secagem de tijolos cerâmicos industriais e estimativa de parâmetros do processo: Uma abordagem concentrada avançada. *Res. Soc. Dev.* **2020**, *9*, e48391211391. [CrossRef]
33. Nascimento, J.J.S.; Belo, F.A.; Lima, A.G.B. Experimental drying of ceramics bricks including shrinkage. *Defect Diffus. Forum* **2015**, *365*, 106–111. [CrossRef]
34. Nascimento, L.P.C.; Silva, S.K.B.M.; Lima, E.S.; Magalhães, H.L.F.; Lima, W.M.P.B.; Gomez, R.S.; Porto, T.R.N.; Lima, A.G.B. Secagem de tijolos cerâmicos argilosos industriais: Uma investigação teórica usando modelos concentrados. *Res. Soc. Dev.* **2020**, *9*, e44291110064. [CrossRef]

35. Silva, A.M.V. Drying of Industrial Ceramic Blocks: Modeling, Simulation and Experimentation. Ph.D. Thesis, Process Engineering, Federal University of Campina Grande, Campina Grande, Brazil, 2018. Available online: http://dspace.sti.ufcg.edu.br:8080/jspui/handle/riufcg/7173 (accessed on 3 December 2022). (In Portuguese).
36. Silva, J.B. Simulation and Experimentation of the Drying of Hollow Ceramic Bricks. Ph.D. Thesis, Process Engineering, Federal University of Campina Grande, Campina Grande, Brazil, 2009. Available online: http://dspace.sti.ufcg.edu.br:8080/xmlui/handle/riufcg/1654 (accessed on 7 December 2022).
37. Tetens, O. Uber einige meteorologische Begriffe. *Z. Geophys.* **1930**, *6*, 297–309.
38. Moran, M.J.; Shapiro, H.N.; Boettner, D.D. *Fundamentals of Engineering Thermodynamics*; John Wiley & Sons: New York, NY, USA, 2010.
39. Monteith, J.; Unsworth, M. *Principles of Environmental Physics: Plants, Animals, and the Atmosphere*; Academic Press: New York, NY, USA, 2013; ISBN 0123869935.
40. Diniz, J.F.B.; Delgado, J.M.P.Q.; Vilela, A.F.; Gomez, R.S.; Viana, A.D.; Figueiredo, M.J.; Diniz, D.D.S.; Rodrigues, I.S.; Rolim, F.D.; Santos, I.B. Drying of Sisal Fiber: A Numerical Analysis by Finite-Volumes. *Energies* **2021**, *14*, 2514. [CrossRef]
41. Fortuna, A.; Fortuna, D.M.; Martini, E. An Industrial Approach to Ceramics: Sanitaryware. *Plinius* **2017**, *43*, 138–145. [CrossRef]